NREL/TP-451-20290 • UC Category: 1262 • DE96000467

Identifying Electronic Properties Relevant to Improving Stability in a-Si:H-Based Cells and Overall Performance in a-Si,Ge:H-Based Cells

Annual Subcontract Report 18 April 1994 – 17 April 1995

J. D. Cohen
University of Oregon
Eugene, Oregon

NREL technical monitor: B. von Roedern

National Renewable Energy Laboratory
1617 Cole Boulevard
Golden, Colorado 80401-3393
A national laboratory of the U.S. Department of Energy
Managed by Midwest Research Institute
for the U.S. Department of Energy
under contract No. DE-AC36-83CH10093

Prepared under Subcontract No. XAN-4-13318-07

November 1995

Available to DOE and DOE contractors from:
Office of Scientific and Technical Information (OSTI)
P.O. Box 62
Oak Ridge, TN 37831
Prices available by calling (615) 576-8401

Available to the public from:
National Technical Information Service (NTIS)
U.S. Department of Commerce
5285 Port Royal Road
Springfield, VA 22161
(703) 487-4650

Printed on paper containing at least 50% wastepaper, including 10% postconsumer waste

PREFACE

This Annual Technical Progress Report covers the work performed at the University of Oregon for the period 18 April 1994 to 17 April 1995 under NREL Subcontract Number XAN-4-13318-07. The following personnel participated in this research program:

NAME	TITLE	WORK PERFORMED
J. David Cohen	Principal Investigator	Program Manager
Fan Zhong	Research Associate	Characterization of Low Gap a-Si,Ge:H Alloys
Daewon Kwon	Research Assistant	Stability Studies of Hot Wire and H-diluted a-Si:H samples
Chih-Chiang Chen	Research Assistant	Characterization of a-Si,Ge:H Alloys, Studies of p-i-n devices.

TABLE OF CONTENTS

LIST OF ILLUSTRATIONS

Page

LIST OF TABLES

EXECUTIVE SUMMARY

Our research during Phase I of NREL Subcontract XAN-4-13318-07 has been focussed on the characterization and evaluation of materials produced by novel deposition conditions and/or methods. The results are based on a variety of junction capacitance techniques: admittance spectroscopy, transient photocapacitance (and photocurrent), and drive-level capacitance profiling. These methods have allowed us to determine deep defect densities and their energy distributions, Urbach bandtail energies and, in some cases, $\mu\tau$ products for hole transport.

First, we have carried out measurements on a-Si,Ge:H alloy samples produced at Harvard University by a cathodic glow discharge process. These samples were found to exhibit nearly an order of magnitude lower defect densities in the high Ge composition range (>50at.% Ge) than alloy samples produced either by conventional glow discharge or photo-CVD deposition. This lower defect density appears to be entirely consistent with a simple defect formation model that was previously found to account for the defect densities in the other types of a-Si,Ge:H samples. Such reduced defect levels in the Harvard samples thus seem to be linked to their larger gaps energy for a given Ge fraction, the different relative energy positions of the defect within the gap, and markedly smaller Urbach energies. However, our measurements also indicated a smaller value of $(\mu\tau)_h$ for these samples than would have been expected given their lower defect densities.

Second, we characterized several hot-wire a-Si:H samples produced with varying hydrogen levels. These samples were evaluated in both their as-grown state as well as a strongly light degraded state. We found that samples with a H content above 10at.% exhibited essentially identical properties to those of conventional glow discharge a-Si:H. However, as the H level was decreased to about 2at.% the electronic properties actually *improved*: the degraded defect level was reduced and Urbach tail was slightly narrower. These changes were accompanied by more than a 0.1eV decrease in optical gap. Therefore, our studies indicate that hot-wire produced a-Si:H, with H levels between 2-5at.%, should lead to mid-gap devices with superior properties.

Finally, we report some results on a-Si:H glow discharge material grown under hydrogen dilution conditions. We confirm that such films exhibit improved stability compared to conventional glow discharge material. We also began some studies to try to gain some insight into the mechanisms responsible for such differences in stability, comparing samples grown with Ar and H dilution as well as a sample that was switched periodically between these two types of gas mixtures during growth. While still very preliminary, our studies point to film strain as playing a primary role for the observed differences in behavior.

1.0 INTRODUCTION

The work carried out in Phase I under NREL Subcontract XAN-4-13318-07 has been focussed on three types of studies. First, we have carried out an extensive evaluation of the basic electronic properties of low mobility gap a-Si,Ge:H alloy films produced at Harvard University by a cathodic glow discharge process. Second, we have investigated the properties of a series of a-Si:H samples with varying hydrogen content produced by the hot-wire deposition process at NREL. These samples were examined both in their as-grown state as well as a light-degraded state. Finally, we have begun a comparison of degradation for glow discharge a-Si:H samples produced with and without hydrogen dilution. In a novel approach we examined samples in which the degree of hydrogen dilution was modulated within a single sample so that possible mechanisms for the difference in degradation rates could be identified.

The experimental results described in this report are based primarily on a variety of junction capacitance techniques: admittance spectroscopy, transient photocapacitance (and photocurrent), and drive-level capacitance profiling. These methods have allowed us to determine deep defect densities and their energy distributions, Urbach bandtail energies and, in some cases, $\mu\tau$ products for hole transport.

For the cathodic a-Si,Ge:H samples we have compared our results with those we obtained previously on alloy samples from other sources. This comparison indicates that the cathodic alloy samples have nearly an order of magnitude lower defect density for a given Ge fraction than the other samples studied previously. However, other differences in behavior have also been found which indicate some basic qualitative differences in electronic properties. For the hot-wire deposited a-Si:H samples we compare the measured properties with high quality glow discharge a-Si:H material. Here we have found nearly identical properties for hot-wire material with hydrogen levels above 10at.%. However, as the hydrogen content of the hot-wire a-Si:H is decreased to 2at.%, the electronic quality of these samples is actually found to improve slightly while the optical gap is decreased. This indicates considerable promise for hot-wire material in solar cell applications.

In the Sections that follow, we first describe the samples studied and then briefly review the experimental techniques employed. In Section 4 we discuss our results concerning the electronic properties of the cathodic a-Si,Ge:H samples. In

Section 5 we present our results on the hot-wire deposited a-Si:H, and in Section 6 our preliminary results on hydrogen diluted a-Si:H. Finally, in Section 7 we summarize our findings and draw some general detailed conclusions.

2.0 SAMPLES

2.1 CATHODIC AMORPHOUS SILICON-GERMANIUM ALLOYS

The a-Si,Ge:H samples were deposited by Paul Wickboldt of William Paul's group at Harvard University by the glow discharge method. However, unlike most other groups, the substrates are attached to the rf electrode, which sustains a negative dc bias during deposition (the cathode).[1] In this method the mixtures of SiH_4 and GeH_4 gases were diluted in H_2. The flow rates of GeH_4 and H_2 were 1.00 sccm and 40.0 sccm, respectively. The SiH_4 flow rate was varied to obtain the different Ge fractions. The temperature of the substrates was kept constant at 225° C, the chamber pressure was maintained at 0.95 Torr, and the rf power density was 1.2 watts/cm^2 for all depositions. The films were grown on both heavily p^+ doped (111) oriented crystalline silicon wafers and on Corning 7059 glass.

We present the general optical and electrical properties of these films deposited at different flow rates of SiH_4 in Table 1. The germanium content of each film was well determined by the electron microprobe method with an error less than 1at.%. The optical gaps E_{04} and E_{03} were measured at Harvard by optical absorption measurements on the glass substrate samples. The dark *ac* conductivity activation energy, E_σ, which we identify with the Fermi energy position, ($E_\sigma \approx E_C - E_F$), was deduced from the C-T-ω measurements for Schottky diode samples (see Section 4).

Table 1: Optical and electrical properties of cathode deposited glow discharge a-$Si_{1-x}Ge_x$:H alloys.

Sample No.	SiH_4 flow (sccm)	Ge content	Bandgap (eV) E_{04}	Bandgap (eV) E_{03}	E_σ (eV)	Thickness (μm) Optical	Thickness (μm) C-T-ω
479	1.60	57.3 at.%	1.57	1.39	0.666	2.83	2.61
478	1.00	67.5 at.%	1.53	1.37	0.645	3.07	3.08
477	0.70	74.5 at.%	1.44	1.30	0.620	2.99	2.77
476	0.37	84.5 at.%	1.40	1.24	0.559	1.97	1.96
427	0.00	100 at.%	1.26	1.12	0.510	—	2.28

Both the optical bandgap and the dark *ac* conductivity activation energy decrease monotonically with increasing Ge content. We also note that E_σ is always less than one-half of E_{04} (or even E_{03}) implying that these alloys are effectively slightly n-type with a Fermi level above mid-gap. The fact that the film thicknesses obtained from capacitance match those derived from the optical absorption measurements indicates the same growth rates for films deposited on the different substrates.

2.2 HOT-WIRE AMORPHOUS SILICON

A set of four a-Si:H films were deposited by Brent Nelson and Eugene Iwaniczko at NREL on stainless using the hot-wire CVD deposition technique. By varying the substrate temperatures during deposition the hydrogen concentration in the films could be varied between more than 10at.% to less than 1at.%.[2] The deposition conditions for the film series is given in Table 2 along with their hydrogen concentrations and thicknesses. The hydrogen concentrations were not actually measured for these samples, but are estimated on the basis of previous film depositions at the same temperatures.

Table 2. Characteristics of hot-wire deposited a-Si:H samples.

Sample No.	Substrate Temp. (°C)	Hydrogen Content (at.%)	Thickness (μm)
HW290	290	10-12	1.45
HW325	325	7-9	1.83
HW360	360	2-3	2.38
HW400	400	< 1	1.69

2.3 HYDROGEN DILUTED GLOW DISCHARGE AMORPHOUS SILICON

Two glow discharge samples were obtained from Rajeewa Arya at Solarex. One was grown under their usual conditions for device quality material (pure silane discharge at a roughly 260°C substrate temperature), and the other was grown under conditions of hydrogen dilution (10:1 H_2:SiH_4 at somewhat lower substrate temperatures). Cells fabricated using the latter material as an i-layer have been found to lead to marked improvement in stabilized performance.

In a preliminary attempt to gain some insight into the mechanisms for improved stability in the hydrogen diluted material, we also carried out a feasibility study on three samples grown in our own glow discharge reactor. We grew one from a gas mixture of 30% SiH_4 diluted in hydrogen, a second sample using 30% SiH_4 diluted in argon, and a third sample in which SiH_4 again accounted for 30% of the mixture, but the dilutant gas was switched from H_2 to Ar every 10 to 15 minutes with a total of 34 layers. This resulted in a 4μm thick sample with a modulation period of about 2300Å. All substrates were heavily p-type crystalline Si and the substrate temperature was 200°C in all cases.

2.4 SAMPLE TREATMENT

Semitransparant palladium Schottky barriers were evaporated on the top of all samples. For the light degradation studies we employed a tungsten-halogen light source either unfiltered or, in cases where spatial uniformity of the degradation was important, used a red filter with a 1.9eV high energy cutoff. Light exposure times were always 100-120 hours. Typical intensities for light exposure were 400mW/cm^2. In some cases we employed intensities of 5W/cm^2 to ensure saturation after 100hours. For these higher intensities we submerged the sample in methanol to maintain the film surface temperature below 65°C.

3.0 EXPERIMENTAL CHARACTERIZATION METHODS

The measurements employed in our studies rely on a small set of experimental techniques which have all been described previously in some detail. They consist of (1) admittance spectroscopy as a function of temperature and frequency, (2) drive-level capacitance profiling, and (3) transient photocapacitance taken together with transient junction photocurrent spectroscopy. For the purpose of this report we will describe each method only very briefly and review what kind of information is obtained from each type of measurement.

3.1 ADMITTANCE SPECTROSCOPY

Our Schottky diode samples contain a depletion region which is characterized as a function of temperature and frequency before we undertake the more sophisticated capacitance based measurements described in Sections 3.2 and 3.3

below. Such measurements provide us with an estimate of our film thickness (the temperature independent region at low T is simply related to the geometric thickness, d, by the formula $C = \varepsilon A/d$), and an Arrhenius plot of the frequency of the lowest temperature capacitance step (or conductance peak) *vs.* 1/T provides us with the activation energy of the ac conductivity, E_σ, which we identify with the Fermi energy position: $E_\sigma = E_C - E_F$.[3] These admittance measurements also give us an indication of the quality of our Schottky barriers which allow us to pre-screen our samples for further study.

3.2 DRIVE-LEVEL CAPACITANCE PROFILING

The drive-level capacitance profiling method has been described in detail in many publications [4,5]. It is similar to other kinds of capacitance profiling in that it provides us with a density vs. distance profile; however, this particular method was developed specifically to address the difficulties encountered in interpreting capacitance measurements in amorphous semiconductors. In this method we monitor the junction capacitance both as a function of DC bias, V_B, and as a function of the amplitude of the alternating exciting voltage, δV. One finds that to lowest order this dependence obeys an equation of the form:

$$C(V_B, \delta V) = C_0(V_B) + C_1(V_B)\,\delta V + \ldots$$

and that the ratio

$$N_{DL} \equiv \frac{C_0^3}{2q_e\,\varepsilon A^2\,C_1}$$

is directly related to an integral over the density of mobility gap defect states:

$$N_{DL} = \int_{E_c - E_e}^{E_F^o} g(E)\,dE$$

Here E_F^o is the bulk Fermi level position in the sample and E_e depends on the frequency and temperature of measurement:

$$E_e(\omega,T) = k_B T \log(\nu/\omega)$$

Thus, by altering the measurment temperature (or frequency) we obtain information about the energy distribution of the defects and, by altering the applied DC bias, we can vary the spatial region at which we detect the defects in the sample. That is, we can spatially profile the defects as a function of the position from the barrier interface.

In our current studies we typically measured 10 or 100Hz profiles for a series of temperatures between 320K to 360K. These data usually indicated a clear upper limit for N_{DL} which, we have shown [6], is equal to roughly one half the total defect density in these samples. This thus provides us with a quantitative measurement of the deep defect levels. In addition, because of the profiling information also obtained, we are able to assess the spatial uniformity of the electronic properties in these samples.

3.3 TRANSIENT PHOTOCAPACITANCE AND PHOTOCURRENT

The methods of junction transient photocapacitance and photocurrent have been discussed by us in great detail recently in the literature [7,8,9] and also in previous NREL reports. They represent types of sub-band-gap optical spectroscopy and provide spectra quite similar in appearance to PDS derived sub-band-gap optical absorption spectra or to CPM spectra. Instead of detecting absorbed energy, however, our photocapacitance and photocurrent transient methods detect the optically induced change in defect charge within the depletion region. However, unlike the CPM method, both of our junction based techniqes are not greatly influence by the free carrier mobilities since, once an electron (or hole) is optically excited into the conduction (valence) band it will either totally escape the depletion region on the slow timescale of our measurement (0.1 to 1s) or be retrapped into a deep state and not escape. In most cases we assume that almost all of the optically excited majority carriers (electrons) *do* escape but, in general, only a fraction of the minority carriers (holes).

Because the photocapacitance and photocurrent measurements have different sensitivities to the loss of electrons *vs*. holes from the depletion region, a detailed comparison of the two kinds of spectra can be used to disclose the escape length of the holes.[8,10] This allows us to estimate the hole $\mu\tau$ products for these samples. In these experiments the parameter τ is identified as a deep trapping time, *not* a recombination time. We are also able to distinguish whether optical excitation of defect states comes about because of the excitation of trapped electrons to the conduction band or because of the excitation of valence band electrons into an empty mobility gap state. This ability to distinguish electron from hole processes is unique among all the various types of sub-band-gap optical spectroscopies.

4.0 CATHODIC AMORPHOUS SILICON-GERMANIUM ALLOYS

To determine the mid-gap defect densities in the cathodic a-$Si_{1-x}Ge_x$:H samples, we carried out drive-level capacitance profiling measurements at 100Hz for a series of temperatures between 290K and 350K. In Fig.1(a) we display typical drive-level capacitance profiling data for the sample with x = 0.57. Unlike previous a-Si,Ge:H samples studied in this fashion, the drive-level density, N_{DL}, did not exhibit any obvious temperature dependence for these samples. For comparison, we plot in Fig.1(b) the temperature variation of N_{DL} for a sample in a similar composition range (x = 0.5) obtained from United Solar Systems Corporation.[11] There are, we believe, two reasons that N_{DL} might be temperature independent for the cathodic samples. First, the bulk Fermi level $E_F{}^o$ may be very close to the quasi Fermi level in deep depletion. In this case, we would be probing the entire deep depletion charge density at even the lowest measurement temperature so that N_{DL} already has its maximum value at 320K. Second, there may be a narrow defect band lying at or above $E_F{}^o$. In that case the capacitance profiling would only show us the portion of the defect band lying below $E_F{}^o$. Thus, the increment of N_{DL} with temperature would be extremely small. Either of these situations imply that we may only be profiling a limited region of the total deep defect band.

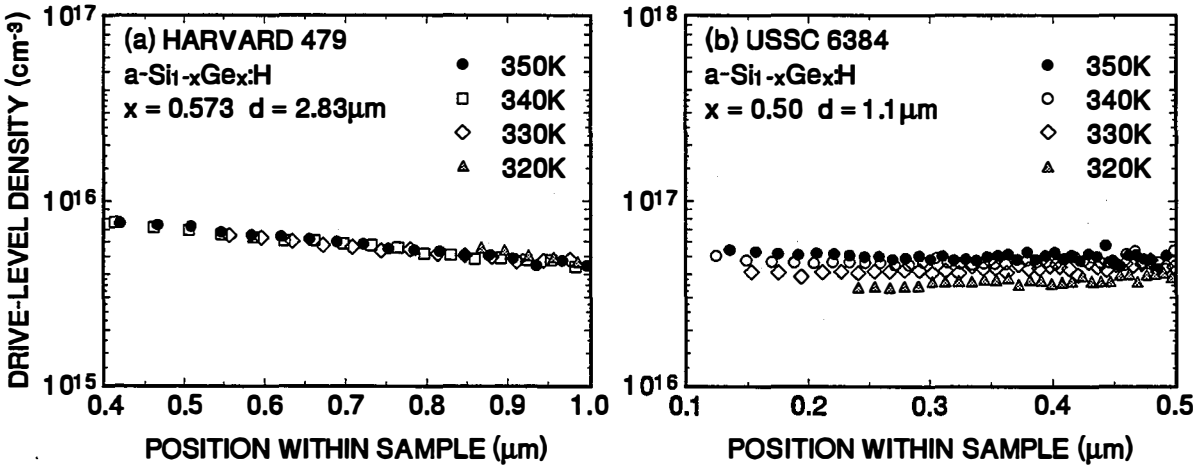

FIG. 1. (a) Temperature independent drive-level density of a cathode deposited sample, (b) an example of the temperature dependent drive-level density of a USSC sample [11].

In Fig. 2 we plot the measured values of N_{DL} *vs.* the Ge content determined for these cathothic alloys along with results from our previous studies of photo-CVD a-Si,Ge:H samples obtained from the Institute for Energy Conversion (Delaware) [12] and the glow discharge provided to us by United Solar Systems.[11] For both these previous series of samples we believe that the limiting value of N_{DL} is indeed providing us with an accurate estimate of the total density of the mid-gap defect band. Although N_{DL} for the cathode deposited glow discharge samples is observed to increase with germanium content in a fashion similar to both the IEC and USSC samples, its value is *almost one order of magnitude lower* than the trend line at high Ge composition indicated for the other a-Si,Ge:H samples.

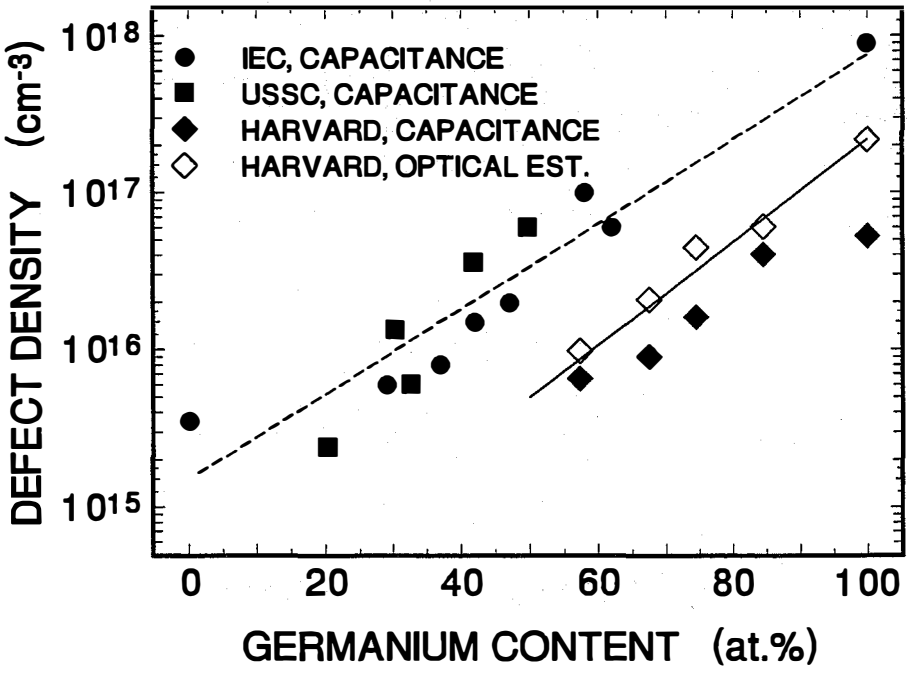

FIG. 2. . A comparison of the total defect densities vs. Ge content for the a-Si,Ge:H alloys from three sources: photo-CVD samples produced at IEC at University of Delaware [12], glow discharge samples produced at USSC [11], and the cathodic glow discharge samples produced at Harvard. The solid symbols are the experimental defect densities determined by drive-level profiling, the open symbols are the defect density estimated from sub-band-gap optical spectra. The dashed lines are the predicted dependence using the spontaneous bond breaking model, assuming a Urbach energy of 53 meV and a ΔE of 0.3eV for the IEC and USSC samples, a narrow Urbach energy of 45meV and a slight larger value of ΔE (0.38eV) for the cathode deposited samples.

To determine the energy positions of the deep defect bands in the mobility gap, we carried out transient photocapacitance and photocurrent measurements on these samples. In Fig. 3 we compare such a pair of spectra for one USSC sample (with x=0.50) with one cathodic a-$Si_{1-x}Ge_x$:H sample (with x=0.57) measured under identical conditions. In all of the IEC and USSC samples we observe a significant deviation between the photocapacitance and photocurrent spectra obtained at higher temperatures similar to that shown in Fig. 3(b). As we discussed in Section 3.3 and elsewhere [8,10], the deviation in the bandtail region is due to contribution of hole processes which decrease the relative magnitude of the photocapacitance signal. The additional somewhat larger deviation near 1.0eV is due to the excitation of valence band electrons into an unoccupied defect level within the mobility gap. In contrast, in Fig. 3(a), we find that there is a nearly constant ratio between the photocurrent and photocapacitance spectra for that sample throughout the entire optical energy regime (0.6eV < $h\nu$ < 1.4eV). This means that the displacement of each hole is sufficiently small that it has very little effect on the transient signals. The most straightforward conclusion would be that the hole $\mu\tau$ products for the cathodic a-Si,Ge:H samples are significantly lower than for the IEC or the USSC samples.

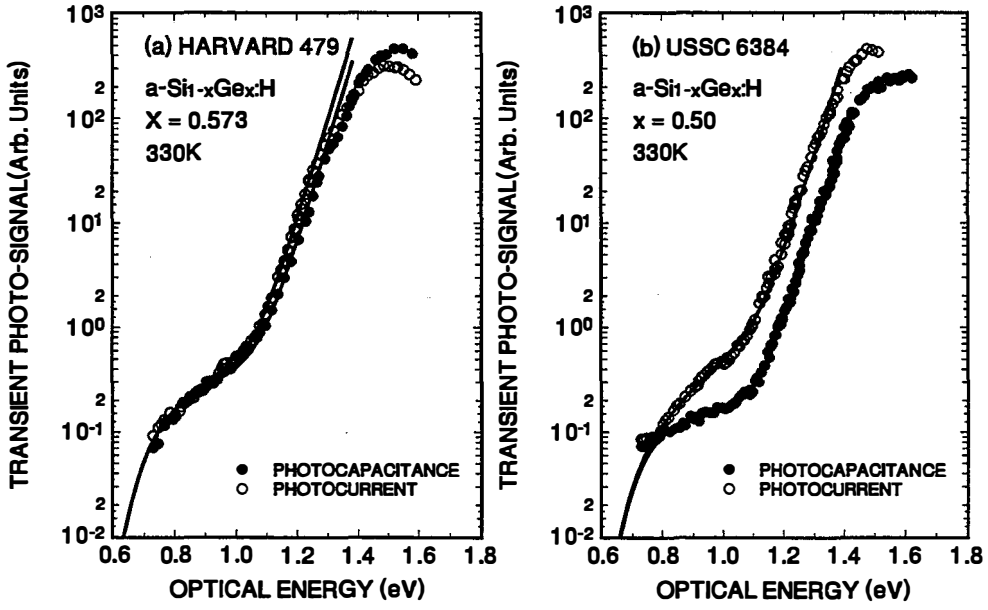

FIG. 3. Pairs of photocapacitance and photocurrent transient spectra for two a-Si,Ge:H samples taken at 330K. These spectra have been aligned to coincide at the lowest optical energies. The marked difference between the two spectra in (b) can be attributed to minority carrier processes.

This interpretation, however, is a bit of an oversimplification. We have previously presented a detailed analysis [8,10,11] by which one can estimate the hole $\mu\tau$ products from the ratio, R, of the photocapacitance to the photocurrent signals in the bandtail energy region (relative to the ratio of the signals in the lowest energy regime which is defined to be unity). Specifically one has:

$$(\mu\tau)_h = \frac{\varepsilon}{q_e N^+} \log\left[\frac{R+1}{2R}\right] \qquad (3)$$

where ε is the dielectric constant, q_e is the electron charge, and N^+ is the charge density in deep depletion. This last quantity is a critical component because it sets the magnitude of the electric field distribution in the depletion region which determines how far a carrier will move within a deep trapping time, τ.

A close examination of the data for the two samples in Fig. 3 indicates that the ratio, R, in the bandtail region (near 1.2eV) between the photocapacitance and photocurrent signals is roughly 0.1 for the USSC sample *vs.* 0.6 for the Harvard sample. The charge density in deep depletion, which is given to us directly from our measurement of N_{DL}, is 5×10^{16} cm^{-3} and 6×10^{15} cm^{-3} for the two samples, respectively. Thus we obtain values of $(\mu\tau)_h$ from Eq. (3) of 2.3×10^{-10} cm^2/V for the USSC sample and 3.2×10^{-10} cm^2/V for the Harvard sample. The error is roughly $\pm$20% in the first case and somewhat larger, $\pm$50%, in the second case (due to difficulty in determining R very accurately when the difference between the spectra is so small). Thus, to within the experimental uncertaintly, the $\mu\tau$ products for Harvard samples appears to be quite comparable to those for the a-Si,Ge:H samples from other sources.

However, such a result is nonetheless quite surprising. The $\mu\tau$ products that we obtain from this type of measurement are indicative of deep trapping processes since they must limit the escape distance for a carrier on roughly a one second time scale. Thus, if the deep defect density is really nearly an order of magnitude lower, then $\mu\tau$ products should be correspondingly greater. Indeed, we had previously found that the product $(\mu\tau)_h N_D$ is nearly constant in the photo-CVD a-Si,Ge:H material over an very large range of Ge concentration [8]. Therefore, the comparable values of $(\mu\tau)_h$ for similar Ge content for the cathodic alloy samples really does indicate a fundamental difference in their properties compared to other types of a-Si,Ge:H material.

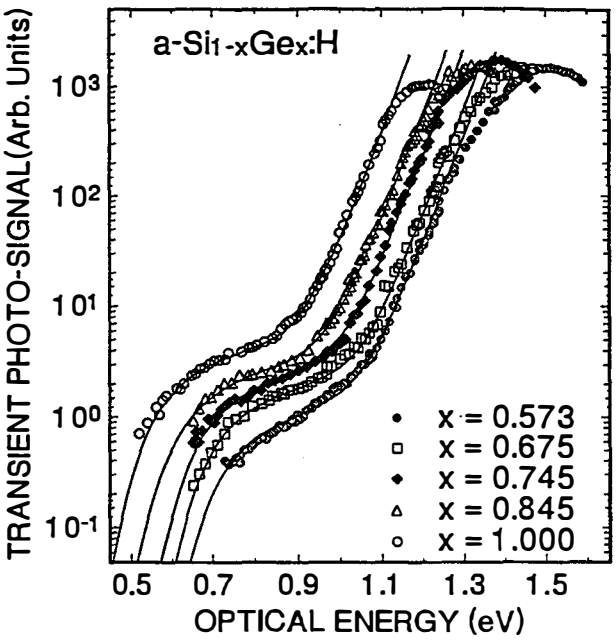

FIG. 4. Sub-band-gap optical spectra for the cathode deposited samples with Ge content between 57 and 100 at.%. The thin solid lines drawn through each spectrum indicate fits based upon an exponential Urbach tail and a Gaussian shaped defect band.

In Fig. 4 we display the sub-band-gap spectra for the entire series of cathodic a-Si,Ge:H samples studied. In all cases there is only a very small difference between the photocapacitance and the corresponding photocurrent spectra. Assuming constant optical matrix elements for bandtail transitions and the deep defect band related transitions we are able to fit these spectra using a single Gaussian deep defect band and a valence band tail of constant slope. (We also assume a constant density of states for the conduction band.) The result of these fits is shown by the thin solid lines drawn through the data points for each curve in Fig. 4. The Urbach energies deduced in this manner are found to be quite small for the cathodic samples, lying close to 45meV in all cases. (For the pure a-Ge:H sample the Urbach energy was determined to be 43meV). From our fitting, we also deduce a broad Gaussian shaped defect band, with width parameter, σ, of 0.2eV, lying about 40meV above the mid-gap energy for each sample.

In Fig. 5 we plot the energy positions of this single optical defect band along with the two optical defect bands obtained from fitting the optical spectra for the IEC and USSC samples. As we discussed above, the second defect transition is not evident in the Harvard samples; however, the minimal hole signal might make the second transition difficult to identify even if it were present. We note that the FWHM of the midgap optical defect band for the cathodic samples is almost twice as large as those of the IEC and USSC samples and the energy positions are somewhat shallower than those of the IEC and USSC samples.

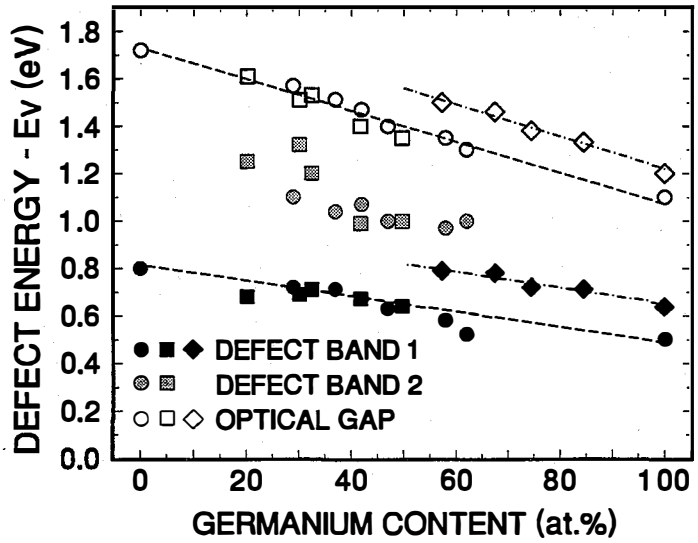

FIG. 5. Energy positions (with respect to E_V) of the defect bands deduced from the sub-band-gap optical spectra for the cathode deposited samples (diamonds) compared with those determined for the IEC photo-CVD samples (circles) [12] and the USSC conventional glow discharge alloy samples (boxes) [11]. The optical gaps for each of the samples is also shown for reference [13].

These spectra can be employed to help verify the low defect densities obtained for the cathodic samples from the drive-level capacitance profiling measurements discussed above. By normalizing the integral of the deduced Gaussian band with the integral of the valence bandtail states we can assign a total defect density to the optical defect band. We assume that the density of valence bandtail states is the same for all these samples since they all exhibit the same Urbach tail slope and use a value of 2×10^{21} cm^{-3} eV^{-1} for the density of states at the valence band mobility edge. Thus, the integrated number of defect states for the valence bandtail is roughly 10^{20} cm^{-3}. Comparing the integral of the defect band with this value provides our estimate for the total density of deep defects. This method has been applied to optical spectra of pure a-Si:H and provides excellent agreement with defect densities derived from drive-level capacitance profiling for those samples [14]. The results of this estimate from the optical spectra are included in Fig.2. We see that the optical estimates for the cathode deposited samples are higher than their drive-level densities by about a factor of 2. This indicates that the drive-level densities may, indeed, providing us with a slight underestimate of the defect density. However, even the larger optical estimates of the defect densities for these cathode deposited samples are substantially lower than the trend line established for the a-Si,Ge:H samples from the other sources.

Both the drive-level densities and the estimates from optical spectra indicate that the as-grown defect densities increase exponentially with increasing the Ge content in the cathode deposited alloys (see Fig.2). Such a trend is consistent with the "spontaneous bond breaking" model [15] which has been used successfully to predict the dangling bond defect density in the a-Si,Ge:H samples from the other sources (see the dashed line in Fig.2) [11,12]. In this model, dangling bonds are thought to be created spontaneously during growth from bandtail states lying beyond a certain demarcation energy above the valence band edge; i.e., "weak bonds". Such a model predicts that the number of dangling bonds will depend solely on the slope of Urbach tail, E_u, and the demarcation energy, E_{db}, relative to the valence band mobility edge. Specifically, if the valence bandtail is described by $N_{tail}(E) = N^* exp(-(E-E^*)/E_u)$, where $N^* \cong 10^{21}\ cm^{-3}$ is the density of states at $E^* \approx E_v + 0.15eV$, then the number of defects created during growth will be:

$$N_D = \int_{E_{db}}^{\infty} N_{tail}(E)dE = E_u N^* \exp(-(E_{db} - E^*)/E_u) \qquad (4)$$

The value of E_{db} is obtained by subtracting an energy of order the defect half-width (the standard deviation, σ, of the Gaussian distribution describing the defect band) from the energy position of the defect band. From Fig.5 we can deduce that the defect position vs. Ge content obeys the relation E_D-$E_V = E_{opt}/2 - 50meV$ for the IEC and USSC samples, and E_D-$E_V = E_{opt}/2 + 40meV$ for the cathode deposited samples. This implies, to a first approximation, that we should have the following relation between defect densities and optical bandgap:

$$N_D = 10^{21} E_u \exp(\Delta E / E_u)\exp(-(E_{opt}/2E_u)) \qquad (5)$$

where ΔE is the sum of $E^* - E_V$, a quantity proportional to the width of the defect band, and the offset between the defect position and midgap. We found a good agreement with the values of the optical estimates using a ΔE of about 0.38eV, which is slightly larger than its value for the IEC and USSC samples (in those cases ΔE is about 0.3eV). This difference of about 80 meV for ΔE comes from the different energy positions of the defect band in the mobility gap between the cathode deposited samples and the IEC and USSC samples. We plot the measured vs. the calculated values for N_D in Fig. 6, and also have included the predicted trends as the dashed lines in Fig. 2. It is clear from Fig. 6 that the optical estimates of cathode deposited samples lie on the same trend line as the IEC and USSC samples. This indicates that the lower defect densities in the cathode deposited samples can be understood within such a model as arising from the different relative position of the defect band within the gap for these samples, their larger optical gap for a given Ge content, and their lower Urbach energies.

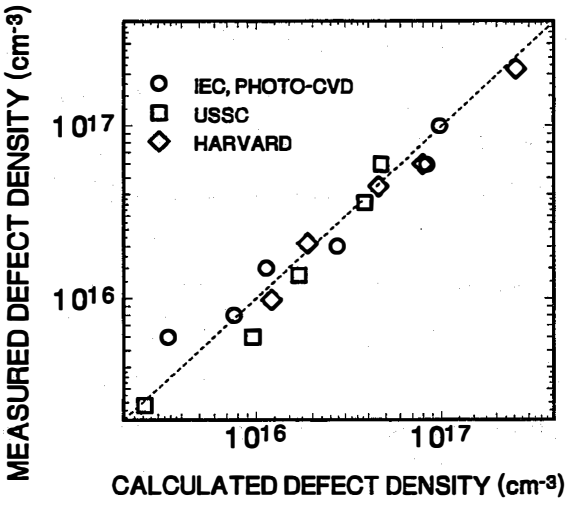

FIG. 6. Measured vs. calculated values of deep defect densities for a-Si,Ge:H alloy samples from various sources. The measured values plotted were obtained from drive-level capacitance profiling except for the cathodic samples where they were estimated from the sub-band-gap optical spectra. The calculated values were obtained from Eq. (5).

Summarizing our experimental results to date on the Harvard cathodic a-Si,Ge:H alloys, we have found that the main features of the mobility gap structure include: (1) a very small Urbach energy, (2) a single broad deep defect band of optical transitions, and (3) a substantially lower defect density compared to other types of alloys in the Ge-rich composition range. It is tempting to associate such qualities with the superior microstructure recently inferred from small angle X-rays scattering (SAXS) studies on the cathode deposited alloy samples [16].

5.0 HOT-WIRE DEPOSITED AMORPHOUS SILICON

Several groups have now reported device-quality a-Si:H films produced by the hot-wire growth technique.[2,17,18] We characterized the electronic properties of NREL deposited hot-wire a-Si:H using transient photocapacitance spectroscopy and also by drive-level capacitance profiling. A comparison of the transient photocapacitance spectra for three hot-wire samples with very different hydrogen levels is displayed in Fig. 7. We then followed the same procedure as described in Section 4: we fit the sub-band-spectra to a density of states consisting of an exponential band tail with slope E_U plus a Gaussian shaped deep defect band. The results of these fits are shown as the thin solid lines in Fig. 7. In all cases the deep defect band was located at an energy of 0.85eV below E_C with a width parameter, σ, of 0.18eV.

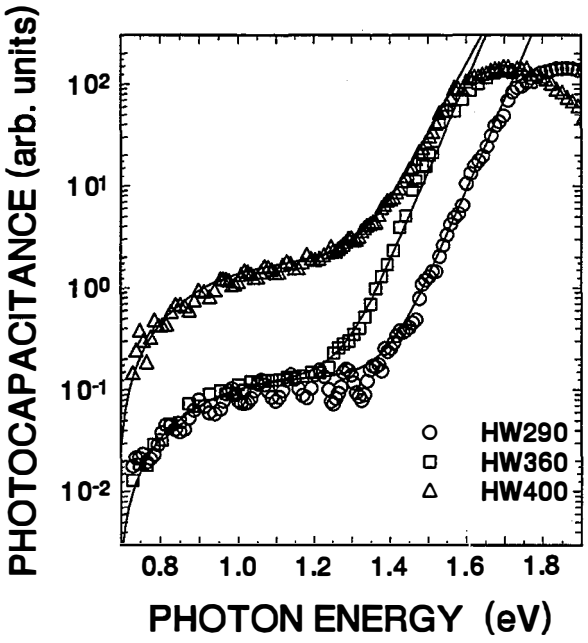

FIG. 7. Comparison of the transient photocapacitance spectra in the as-grown state for three different substrate temperatures. All spectra were obtained at 340K. The solid lines indicate spectra calculated from a density of states consisiting of a Gaussian shaped defect band plus an exponential bandtail.

These data clearly indicate a significant reduction in the optical gap for the samples grown at higher substrate temperatures. A value of E_{04} was estimated from the fall off of the signal at higher optical energies which indicated the degree of attenuation of the probe light through the thickness of the sample. These values, together with the derived Urbach energies are summarized in Fig. 8. We see that the Urbach energy remains roughly constant until the hydrogen content falls below 2at.% while, at the same time, the optical gap is decreased by more that 0.1eV. This indicates that a significant reduction in optical gap can be achieved without introducing excess structural disorder into these hot-wire samples.

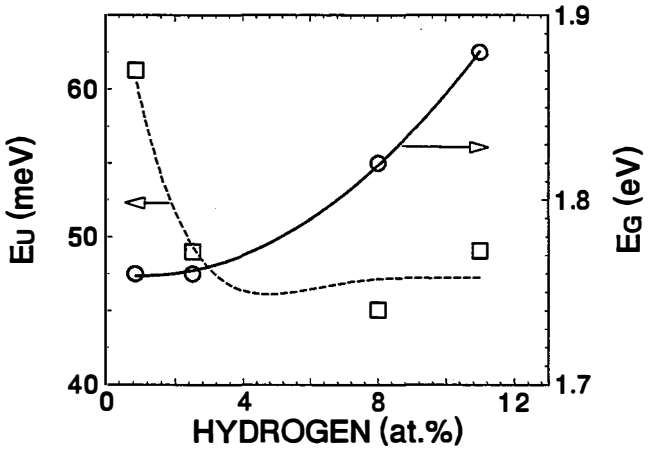

FIG. 8. Variation of the optical gaps and the Urbach energies vs. Hydrogen content determined from the sub-band-gap photocapacitance spectra for the hot-wire a-Si:H samples.

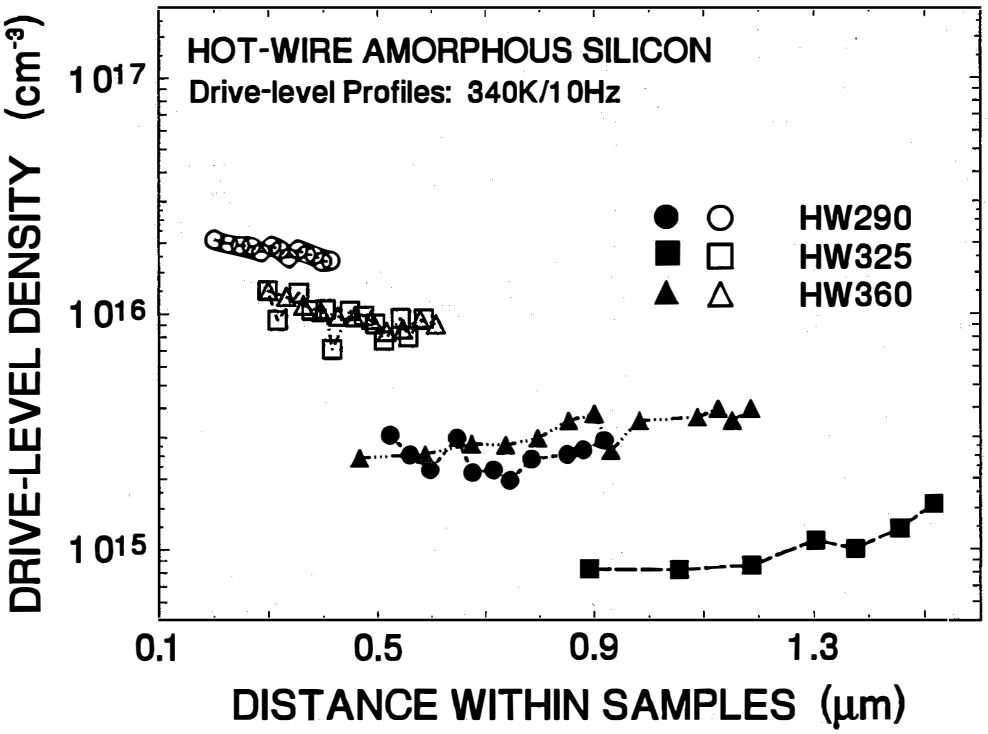

FIG. 9. Drive level capacitance profiling data for three hot-wire a-Si:H samples before (solid symbols) and after (open symbols) light soaking. These data were obtained at 340K using a measurement temperature of 340K. The indicated profiling densities should be multiplied by a factor of 2 to obtain an estimate of the total deep defect density.

In Fig. 9 we present the results of capacitance profiling measurements on three hot-wire samples with hydrogen content between 2.5 to 12at.% (the lowest H sample was too defective to be measured in this fashion). Results are shown both for the as-grown states and after 110 hours of light soaking at 5 Watts/cm^2 unfiltered tungsten-halogen light. The sample with 2.5at.% H was also examined after 250 hours exposure with no apparent difference, indicating that saturation conditions have been reached. In Fig. 10 we summarize the deduced defect densities in the as-grown state both for the capacitance measurements and also as estimated from the defect band region of the optical spectra obtained from Fig. 7. We find good agreement in all cases where both types of measurements could be performed. This indicates that the estimate of 1.5×10^{17} cm^{-3} defects from the optical spectrum for the lowest H sample is probably fairly accurate. Such a large defect density is certainly not surprising for a sample with less than 1at.% H. However, it is quite surprising that the sample with roughly 2.5at.% H should exhibit a total defect density of less than 1×10^{16} cm^{-3}.

In Fig. 11 we compare the defect densities for the samples before and after light degradation. This figure indicates that the stabilized density of deep defects is actually lowest for the sample near 2.5at.% even though its initial defect density is slightly higher. In general we can state that the highest H sample actually exhibits properties nearly identical to conventional glow discharge a-Si:H while the hot-wire samples with H levels near 2at.% exhibit slightly superior properties: a lower stabilized defect density plus a narrower Urbach edge. Given the fact that these samples also exhibit a slightly lower optical gap, they seem potentially quite promising for incorporation into cells as a superior midgap material.

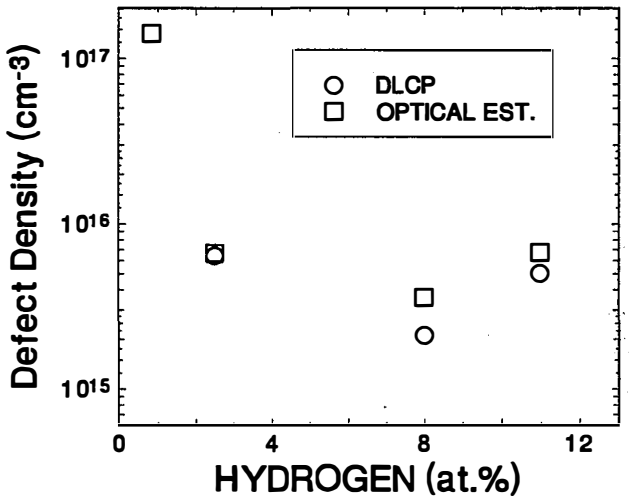

FIG. 10. Comparison of the total deep defect densities obtained both from the capacitance profiling data of Fig. 9 (obtained by doubling the values of the DLCP data at 340K), and the sub-band-gap photocapacitance spectra of Fig. 7. Note the good agreement between the estimates from these two types of experimental data.

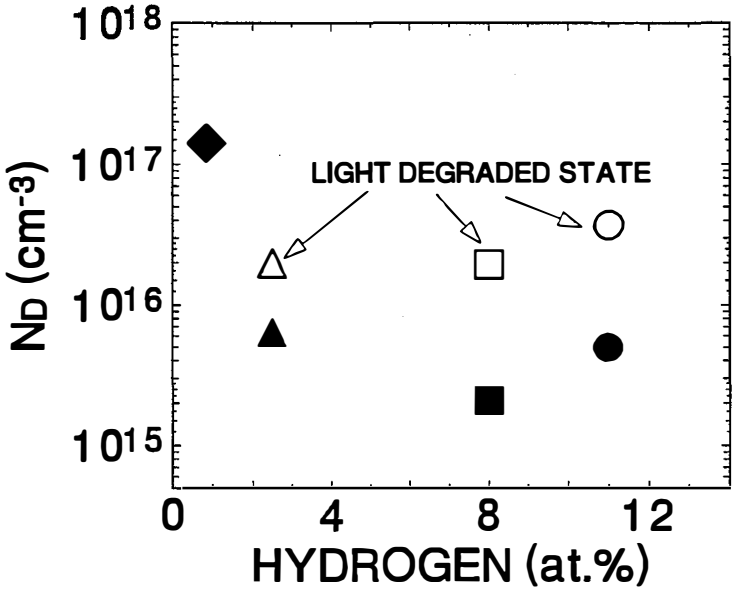

FIG. 11. Comparison of defect densities before and after light soaking. Note that these data indicate that the best stabilized properties are realized for hot-wire samples containing roughly 2at.% hydrogen.

6.0 STABILITY OF HYDROGEN DILUTED GLOW DISCHARGE a-Si:H

We have carried out some preliminary studies comparing glow discharge a-Si:H samples grown with hydrogen dilution with material grown without hydrogen dilution. A pair of samples was received from Solarex Corporation [19], one grown by their conventional glow discharge process, and the other grown under conditions of high hydrogen dilution. We evaluated the degraded defect densities in these two samples using both of our standard methods: via drive-level capacitance profiling and by photocapacitance spectroscopy. Both samples were light soaked for 90 hours at 400mW/cm^2 before evaluation.

Results from the capacitance profiling measurements are shown in Fig. 12 and those from photocapacitance are shown in Fig. 13. Both measurements indicate that the hydrogen diluted sample degraded to a deep defect density that was nearly a factor of 2 lower than the normal glow discharge a-Si:H film. That is, the Solarex hydrogen diluted material definitely appears to be more stable against light induced defect formation.

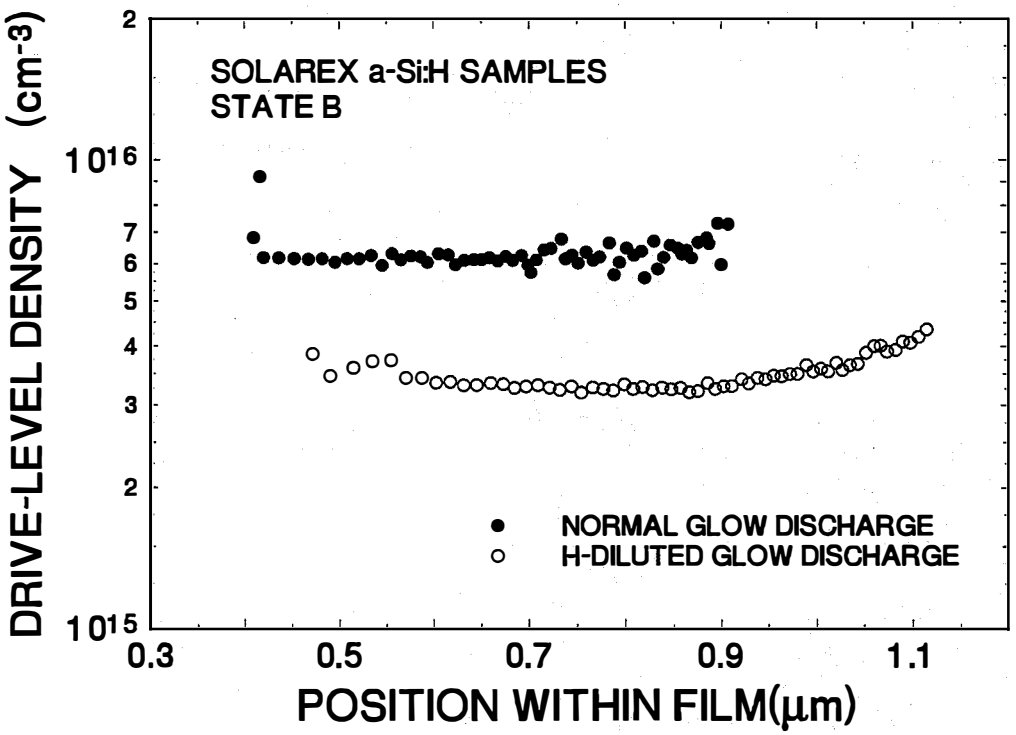

FIG. 12. Drive-level deep defect profiles for two a-Si:H samples in light-degraded states. These 500Hz capacitance profiles measured at 360K should be multiplied by a factor of 3 to yield an estimate of the total defect density [6]. The sample grown with hydrogen dilution shows a significantly lower concentration of defects.

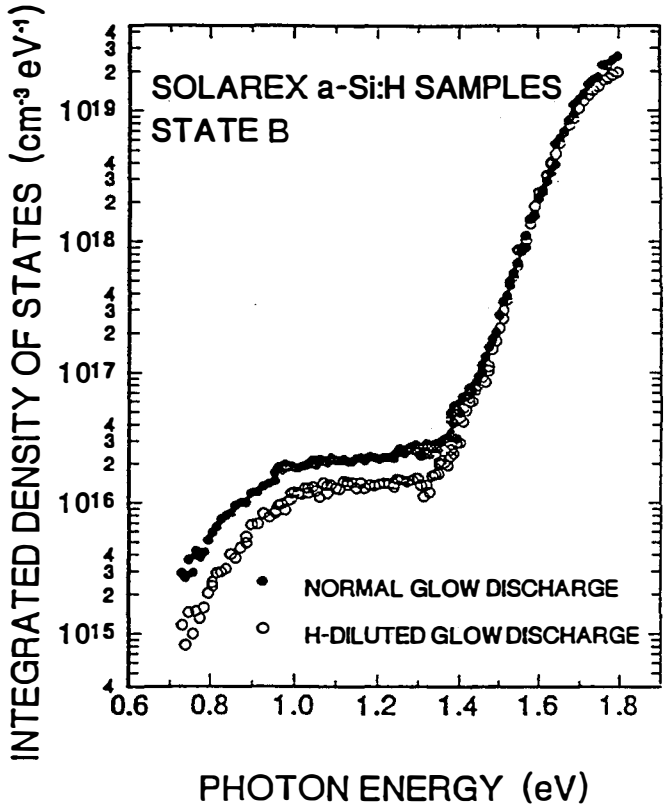

FIG. 13. Photocapacitance sub-band-gap spectra for the same two samples in their light-degraded states. The difference in magnitudes of the deep defect portion of these spectra agrees with that indicated in the drive-level profiling measurements shown above.

Finally, we are attempting to gain some insight into the possible mechanisms responsible for the above differences in susceptibility to the light-induced degradation. A somewhat unique approach is being explored: evaluating the differences in the degradation between hyrogen diluted and normal material within a single a-Si:H film. Our quite preliminary results are described in detail below.

We deposited three kinds of a-Si:H films on heavily doped p^+ crystalline silicon substrates by the RF glow discharge technique at 200 °C: One was a multilayer sample and the other two were homogeneous samples. One homogeneous sample was deposited from a mixture of silane and argon gases and the other from a mixture of silane and hydrogen gases. Each layer in the multilayer sample was grown from the silane gas diluted alternately with either argon or hydrogen gas. The dilution ratio of the silane gas to the total gas mixture for all cases was identical such that the silane gas accounted for 30 % of the volume fraction of the total gas flow. Each argon (hydrogen) dilution layer in the multilayer sample was grown for 15 (10) minutes with a total of 34 layers in all for

a total growth time of 7 hours and 5minutes. This resulted in a 4 μm thick sample, giving a modulation period of about 2300 Å.

After the growth, palladium Schottky barriers were evaporated on top of the amorphous films. A series of light soaked states were obtained by exposing the samples to about 400 mW/cm^2 band gap light for a determined period of time at each step. Following more than 100 hours of light soaking, and saturation of the deep defect densities, a series of partially annealed states were attained by annealing the samples at a series of increasing temperatures for 10 minutes duration at each temperature. Final post-annealed states were obtained by annealing the samples for 30 minutes at 520 K (the same temperature for preparing the initial state A samples).

The spatial dependence of the defect densities were examined by our drive-level capacitance profiling method. Figure 14 shows such data for several different states for the three samples. We observe that the multilayer sample shows a clear variation in its defect densities vs. distance in state A and also after short light exposure times (up to about 1 hour). The spatial period is exactly what we expected from the modulated growth conditions. Moreover, the high defect value of multilayer sample matches the value of the homogeneous hydrogen diluted sample and the low value of multilayer sample matches the value of homogeneous argon diluted sample. This means that hydrogen dilution sample has higher density of defects than the argon diluted sample in state A and so does hydrogen diluted layer in multilayer sample.

However, as the illumination time gets longer the defect level of hydrogen diluted homogeneous sample becomes almost the same as the defect level of argon diluted homogeneous sample and the variation of defect of multilayer sample becomes very small. This can be seen in the 5.33 hours illumination data in Fig. 14. This behavior is distinct from what we had observed in the Solarex samples and indicates that the growth conditions for our samples did not match theirs in some significant way. Obviously, this study should be repeated with the Solarex conditions. Nonetheless, we can state that the high and low densities of defects of multilayer sample track well those defect levels of homogeneous samples until the time of light soaking reaches around 11 hours.

Following this level of light exposure, however, something quite unexpected happens. More prolonged light soaking causes the defect level of multilayer sample

to become larger than *either* of the homogeneous samples! Moreover, the higher defect density condition of the multilayer sample persists until the samples are annealed at high temperatures. Only when the multilayer sample is fully annealed (at the same temperature as the original state A) do the defect levels show a clear match to the levels of the fully post-annealed hydrogen diluted sample and that of the argon diluted sample.

The data presented above are relatively unique in that they allow us to begin to distinguish between local and global aspects of light induced defect creation and annealing. "Local" aspects would be those that are controlled by characteristics of the individual sites for stable and metastable defects and their immediate surroundings: non-diffusing impurities, voids, complexes, etc. Examples of "global" aspects would be those that are controlled by free carrier densities, impurities that are able to diffuse over distances comparable to the multilayer distance, and film strain.

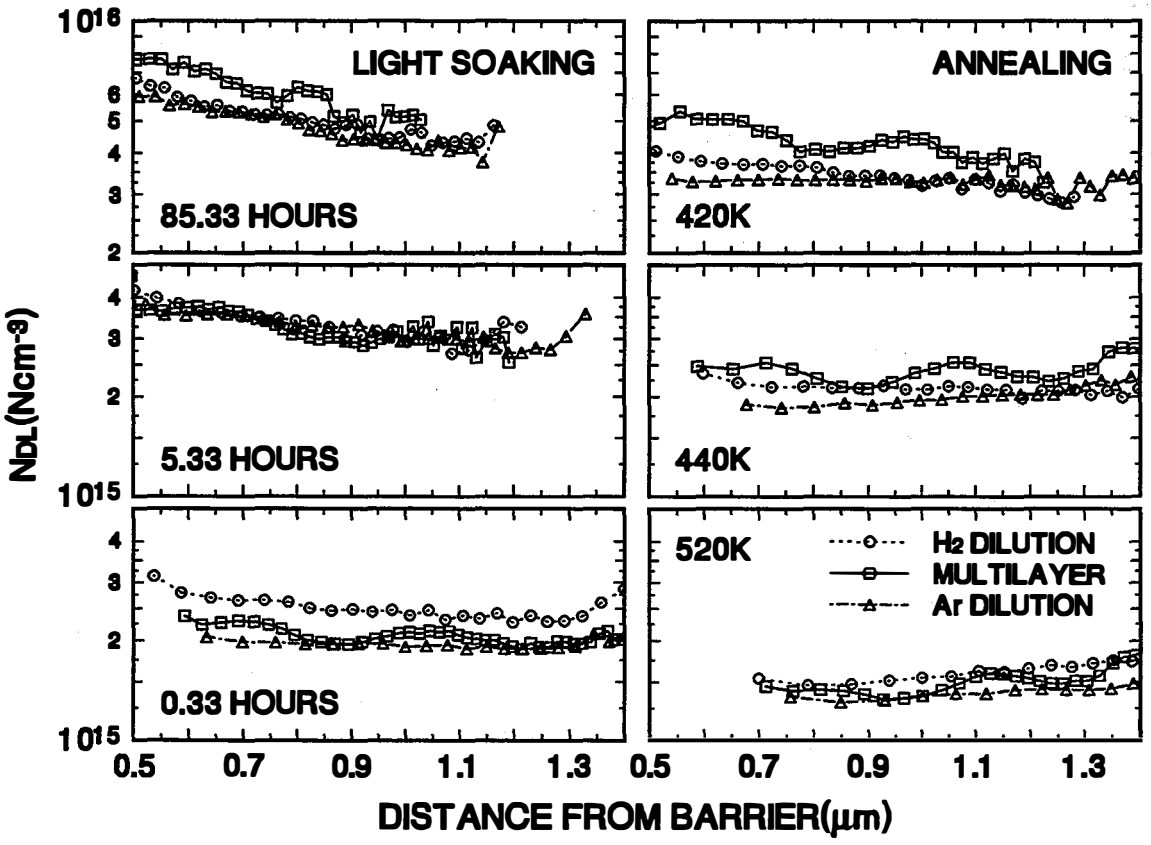

FIG. 14. Drive-level capacitance profiling data for three light soaked states (left) and three post-annealed states (right). The times shown in the left figures are light soaking times and the temperatures shown in the right figures are post-annealing temperatures. Chronologically the left bottom figure is the earliest state and the sequence progresses in a clockwise fashion.

Such local aspects also seem to dominate the metastable defect creation in the earlier stages of light soaking. Unfortunately, because the homogeneous Ar and H_2 diluted films have defect levels which become very similar after a few hours exposure, we cannot be sure whether or not this local character persists. Since carrier recombination is a dominant factor in creating these metastable defects, one would expect to observe a more global aspect to the metastable defect densities; namely, that the multilayer defect density would tend to become more uniform after long periods of light expusure. We will be able to test this in more detail in the future by utilizing component layers whose susceptibility to light induced degredation in homogeneous films exhibit a more pronounced difference.

The most surprising aspect of the defect creation process in our multilayer sample is that the defect density at long light exposure times eventually *exceeds* that of either homogeneous film. This is difficult to understand simply in terms of local or global equilibrium processes. To account for such a result we must identify mechanisms that are peculiar to the multilayer nature of that sample. At present we can offer two possibilities: First, that it involves the separation of free electron and hole carriers and, second, that it is related to an increased level of strain in the multilayer sample. The first of these seems less likely for two reasons: separating holes and electrons should tend to reduce the rate of metastable defect creation. In addition, such a mechanism might be expected to accentuate the differences between the light-induced effects in the different layers.

The second mechanism, that a multilayer sample may have intrinsically a high degree of strain than a homogeneous film of either type, seems more plausible. Indeed, studies relating metastable defect creation to film strain in a-Si:H were reported nearly a decade ago.[20] However, if this is indeed the correct explanation it is then a bit surprising that the state A defect densities do not seem to be affected since these quite accurately reproduce the levels in each of the homogeneous samples. Such a result implies a very different character to the stable vs. the metastable defects and thus seems to contradict a fundamental assumption of defect equilibrium models. Along these lines it is also noteworthy how well the final post-annealing treatment restores the spatial defect variation of the initial state. This again implies a definite local aspect for the stable defects independent of any changes that have occurred as a result of prolonged light exposure and annealing (such as diffusion of H between the layers).

7.0 DISCUSSION

The work carried out during this first phase of our NREL Subcontract has been focused on the characterization and evaluation of materials produced by novel deposition conditions and/or methods. First, we reported results of our measurements on a-Si,Ge:H alloy "cathodic" samples produced at Harvard University. These samples were found to exhibit significantly lower defect densities in the high Ge composition range (>50at.% Ge) than alloy samples produced either by conventional glow discharge or photo-CVD deposition. Moreover, this lower defect density appears to be entirely consistent with simple defect formation models given the differences observed for other aspects of the electronic structure in these samples: a larger gap energy for a given Ge fraction, a different relative energy position of the defect within the gap, and a smaller Urbach energy. It is as yet unclear, however, whether these cathodic alloy samples will lead to a significant improvement in low gap cells. That is, our measurements also indicated a much smaller value of $(\mu\tau)_h$ for these samples than would have been expected given their lower defect densities, and we also found other puzzling qualitative differences. Nonetheless, these cathodic alloys do potentially appear to be quite promising and should definitely be incorporated into test devices for further evaluation.

Second, we reported our results on several hot-wire a-Si:H samples produced with varying hydrogen levels. These samples were evaluated in both their as-grown state as well as a strongly light degraded state. We found that samples with a H content above 10at.% exhibited essentially identical properties to those of conventional glow discharge a-Si:H. However, as the H level was decreased to about 2at.% the electronic properties actually *improved*: the degraded defect level was reduced and the Urbach tail was slightly narrower. (Below 1at.% hydrogen the properties of these hot-wire films were found to deteriorate markedly.) These changes were accompanied by more than a 0.1eV decrease in optical gap. Therefore, our studies indicate that hot-wire produced a-Si:H, with H levels between 2-5at.%, should lead to mid-gap devices with superior properties. Every effort should be made to evaluate this material in test devices.

Finally, we discussed some results on a-Si:H glow discharge material grown under hydrogen dilution conditions. We confirmed that, in terms of deep defect creation, such films exhibited improved stability compared to conventional glow discharge material. We also began some studies to try to gain some insight into the mechanisms responsible for such differences in stability. We compared Ar and H

samples with a sample that was switched periodically between these two types of gas mixtures during growth. While still very preliminary, our studies point to film strain as playing a primary role for the observed differences in behavior. We intend to continue these types of studies during Phase II.

8.0 SUBCONTRACT SUPPORTED PUBLICATIONS

1. Daewon Kwon and J. David Cohen, "Metastable Defect Studies in hydrogen modulated multilayer amorphous silicon", Mat. Res. Soc. Symp. Proc. **336**, 305 (1994).

2. F. Zhong, J.D. Cohen, J. Yang, and S. Guha, "The electronic structure of a-Si,Ge:H alloys", Mat. Res. Soc. Symp. Proc. **336**, 493 (1994).

3. F. Zhong, C.-C. Chen, J.D. Cohen, P. Wickboldt, and W. Paul, "Defect properties of cathode deposited glow discharge amorphous silicon germanium alloys", accepted for publication in the Mat. Res. Soc. Symp. Proceedings.

4. D. Kwon, J.D. Cohen, B.P. Nelson, and E. Iwaniczko, "Effect of light soaking on hot wire deposited a-Si:H films", accepted for publication in the Mat. Res. Soc. Symp. Proceedings.

9.0 REFERENCES

1. W. Paul, J. Non-Cryst. Solids **137&138**, 803 (1991).

2. A.H. Mahan, J. Carapella, B.P. Nelson, and R.S. Crandall, J. Appl. Phys. **69**, 6728 (1991).

3. D.V. Lang, J.D.Cohen, and J.P. Harbison, Phys. Rev. B**25**, 5285 (1982).

4. C.E. Michelson, A.V. Gelatos, and J.D. Cohen, Appl. Phys. Lett. **47**, 412 (1985).

5. K.K. Mahavadi, K. Zellama, J.D. Cohen, and J.P. Harbison, Phys. Rev. B**35**, 7776 (1987).

6. T. Unold, J. Hautala, and J.D. Cohen, Phys. Rev. B**50**, 16985 (1994).

7. J.D. Cohen and A.V. Gelatos, in *Advances in Disordered Semiconductors Vol I: Amorphous Silicon and Related Materials*, ed. by H. Fritzsche (World Scientific, Singapore, 1988), pp. 475-512.

8. J. David Cohen, Thomas Unold, A.V. Gelatos, and C.M. Fortmann, J. Non-Cryst. Solids **141**, 142 (1992).

9. T. Unold, J.D. Cohen, and C.M. Fortmann, Mat. Res. Soc. Symp. Proc. **258**, 499 (1992).

10. A.V. Gelatos, K.K. Mahavadi, and J.D. Cohen, Appl. Phys. Lett. **53**, 403 (1988).

11. For a more detailed discussion of the results of our studies of the electronic properties of a-Si,Ge:H alloy samples produced at United Solar Systems Corp. see NREL Report: TP-451-7163 (1994); also, F. Zhong, J.D. Cohen, J. Yang, and S. Guha, Mat. Res. Soc. Symp. Proc. **336**, 493 (1994).

12. T. Unold, J.D. Cohen, and C.M. Fortmann, Appl. Phys. Lett. **64**, 1714 (1994).

13. For the cathode deposited samples we used an optical gap of E_{04} *minus* 60meV. The corresponding values of the optical gap for the IEC and USSC samples were estimated from their transient photocurrent spectra.

14. D. Kwon, J.D. Cohen, B.P. Nelson, and E. Iwaniczko, Mat. Res. Soc. Symp. Proc., 1995, in press.

15. M Stutzmann, Philos. Mag. B**60**, 531 (1989).

16. D. L. Williamson, Y. Chen., and S.J. Jones, AIP Conf. Proc. **124**, 442 1994).

17. P. Papadopoulos, A. Scholz, S. Bauer, B. Schröder, and H. Oechsner, J. Non-Cryst. Solids 164-166, 87 (1993).

18. E.C. Molenbroek, A.H. Mahan, E.J. Johnson, and A.C. Gallagher, Mat. Res. Soc. Symp. Proc. **336**, 43 (1993).

19. These samples were received courtesy of Rajeewa Arya.

20. M. Stutzmann, W.B. Jackson, and C.C. Tsai, J. Non-Cryst. Solids **77&78**, 363 (1985).

REPORT DOCUMENTATION PAGE

Form Approved
OMB NO. 0704-0188

1. AGENCY USE ONLY (Leave blank)	2. REPORT DATE	3. REPORT TYPE AND DATES COVERED
	November1995	Annual Subcontract Report, 18 April 1994 -17 April 1995

4. TITLE AND SUBTITLE

Identifying Electronic Properties Relevant to Improving Stability in a-Si:H-Based Cells and Overall Performance in a-Si,Ge:H-Based Cells

5. FUNDING NUMBERS

C: XAN-4-13318-07

TA: PV631101

6. AUTHOR(S)

J. D. Cohen

7. PERFORMING ORGANIZATION NAME(S) AND ADDRESS(ES)

Department of Physics and Materials Science Institute
University of Oregon
Eugene, Oregon

8. PERFORMING ORGANIZATION REPORT NUMBER

9. SPONSORING/MONITORING AGENCY NAME(S) AND ADDRESS(ES)

National Renewable Energy Laboratory
1617 Cole Blvd.
Golden, CO 80401-3393

10. SPONSORING/MONITORING AGENCY REPORT NUMBER

TP-451-20290

DE96000467

11. SUPPLEMENTARY NOTES

NREL Technical Monitor: B. von Roedern

12a. DISTRIBUTION/AVAILABILITY STATEMENT

12b. DISTRIBUTION CODE

UC-1262

13. ABSTRACT *(Maximum 200 words)*

This report describes work performed by the University of Oregon focusing on the characterization and evaluation of amorphous semiconductor materials produced by novel deposition conditions and/or methods. The results are based on a variety of junction capacitance techniques: admittance spectroscopy, transient photocapacitance (and photocurrent), and drive-level capacitance profiling. These methods allow the determination of deep defect densities and their energy distributions, Urbach bandtail energies, and, in some cases, $\mu\tau$ products for hole transport. During this phase, we completed out several tasks: (1) We carried out measurements on a-Si,Ge:H alloy samples produced at Harvard University by a cathodic glow discharge process. Measurement indicated a smaller value of $(\mu\tau)_h$ for these samples than would have been expected given their lower defect densities. (2) We characterized several hot-wire a-Si:H samples produced with varying hydrogen levels. Our studies indicated that hot-wire-produced a-Si:H, with H levels between 2–5 at.% should lead to mid-gap devices with superior properties. (3) We reported some results on a-Si:H glow discharge material grown under hydrogen dilution conditions. Preliminary studies point to film strain as playing a primary role for the observed differences in behavior.

14. SUBJECT TERMS

photovoltaics ; solar cells

15. NUMBER OF PAGES

35

16. PRICE CODE

17. SECURITY CLASSIFICATION OF REPORT	18. SECURITY CLASSIFICATION OF THIS PAGE	19. SECURITY CLASSIFICATION OF ABSTRACT	20. LIMITATION OF ABSTRACT
Unclassified	Unclassified	Unclassified	UL